Trop J Nat Prod Res, February 2023; 7(2):2362-2370 ISSN 2616-0684 (Print)
ISSN 2616-0692 (Electronic)

Tropical Journal of Natural Product Research

Available online at https://www.tjnpr.org

Original Research Article

Prediction of a Stable Complex of Compounds in the Ethanol Extract of Celery Leaves (*Apium graveolens* L.) Function as a VKORC1 Antagonist

Aiyi Asnawi[1]*, Marselina Nedja[1], Ellin Febrina[2], Purwaniati Purwaniati[1]

[1]*Faculty of Pharmacy, Universitas Bhakti Kencana, Jl. Soekarno Hatta No.754, Bandung, West Java, 40617, Indonesia*
[2]*Faculty of Pharmacy, Universitas Padjadjaran, Jl. Raya Bandung-Sumedang Km. 21, Jatinangor, Sumedang, West Java, 45363, Indonesia*.

ARTICLE INFO

Article history:
Received 26 December 2022
Revised 27 January 2023
Accepted 03 February 2023
Published online 01 March 2023

ABSTRACT

The vitamin K cycle, specifically the protein VKORC1 (Vitamin K epoxide reductase complex subunit 1), is closely linked to coagulation mechanisms in the body. Disruptions in this cycle will be associated with vascular diseases such as myocardial infarction and stroke. Warfarin is commonly used as an anticoagulant, but it still has side effects in interactions with numerous drug compounds; thus, it is necessary to search for safer candidate compounds. The ethanol extract of celery leaves (*Apium graveolens* L.) has potential anticoagulant activity, but the compound responsible for this activity has not been identified yet. The CADD method has been developed to predict *in silico* a compound's potential to interact with binding sites. This study aimed to predict interactions and obtain a stable complex of the compounds in the ethanol extract of celery leaves, which function as a VKORC1 antagonist. A total of 23 compounds were simulated using Autodock 4.2, and AMBER 18 was then used to simulate the stability of the five compounds with the best interactions. The docking simulation results of 17 test compounds (ligands) yielded five selected compounds, namely *6-isopentenyloxy-isobergapten* (S1), *Heratomin* (S2), *Apigenin* (S3), *Lanatin* (S4), and *Isoimperatorin* (S5), with ΔG values of –9.27, –9.26, –9.22, –9.13, and –8.94 kcal/mol, respectively. The MD simulation continued to produce *6-isopentenyloxy-isobergapten* as the most effective ligand for stabilizing the complex for 100 ns from these five ligands. In conclusion, the *6-isopentenyloxy-isobergapten* from celery leaf has the potential as a candidate anticoagulant, VKORC1.

Keywords: Anticoagulants, Celery Leaves, Molecular Docking, Molecular Dynamics, VKORC1

Introduction

Hemostasis is the process of suddenly stopping bleeding from blood vessels caused by torn blood vessels so that blood can continue to flow to cover the damage that occurs in the blood vessel walls. These events can reduce blood loss when an injury occurs. Coagulation is the occurrence of blood clots, a process in the hemostasis mechanism. When the hemostatic system is unbalanced, it will cause pathological abnormalities, namely, spontaneous bleeding because blood cannot clot, and a thrombus will form, resulting in excessive blockage.[1] The thrombus that forms will cause vascular disease, including myocardial infarction, stroke, and other vascular diseases. Cardiovascular disease is one of the leading causes of death in the world. In 2016, *the World Health Organization* (WHO) noted that there were 56.9 million people who died worldwide due to Ischemic Heart Disease (CHD) and 15.2 million people due to stroke.[2] All treatment efforts are carried out both pharmacologically and non-pharmacologically. One of the drugs used as a therapy to treat vascular disorders due to thromboembolism is an anticoagulant.

Anticoagulants are a class of drugs that can prevent blood clots. It works by binding and converting fibrinogen into fibrin in the blood clotting process.

*Corresponding author. E mail: aiyi.asnawi@bku.ac.id
Tel: +62 22 7830760

Citation: Asnawi A, Nedja M, Febrina E, Purwaniati P. Prediction of a Stable Complex of Compounds in the Ethanol Extract of Celery Leaves (*Apium graveolens* L.) Function as a VKORC1 Antagonist. Trop J Nat Prod Res. 2023; 7(2):2346-2351 http://.www.doi.org/10.26538/tjnpr/v7i2.10

Official Journal of Natural Product Research Group, Faculty of Pharmacy, University of Benin, Benin City, Nigeria.

Anticoagulants also work by inhibiting the function of several factors that play a role in blood clotting, namely by binding to calcium. In addition, another function of anticoagulants is needed to prevent the formation and spread of embolus.[3] Warfarin has been one of the most popular anticoagulant drugs in the world since 1954. This vitamin K antagonist prevents clotting factors VII, IX, X, and II formations. Because of its popularity, warfarin is widely prescribed, reaching 0.5–1.5% of the world's population.[4] Although very popular, warfarin still has drawbacks, namely, having a narrow therapeutic index and interacting with many drugs.[5] Because of this, there is a need for alternative candidate drug compounds that can act as anticoagulants and have fewer adverse effects.

Compounds from herbal plants have been reported to have advantages such as being easy to obtain and isolate and having low side effects. Celery leaves (*Apium graveolens* L.) are a plant that has many benefits. In Indonesia, celery leaves are not only used as a complement to vegetables but also as a traditional medicinal ingredient. According to previous research, celery has antidiuretic, antihypertensive, anti-inflammatory, antioxidant, antirheumatic, and anticoagulant properties. The chemical compounds contained in celery leaves are flavonoids, saponins, tannins, essential oils, vitamins A, B, and C, asparagine, calcium, sulfur, and phosphorus. All of these ingredients are found in all parts of the celery plant.[6] Other studies also reported that the ethanol extract from celery leaves was able to replace EDTA (*Ethylene Diamine Tetraacetic Acid*) as an anticoagulant in calculating the number of platelets.[7] Testing the ethanol extract of celery leaves at a concentration of 50% had the same results as the standard anticoagulant, EDTA. It is worthwhile to conduct additional research into the active components of celery, which are responsible for its anticoagulant activity. The traditional methods for finding functional native products rely heavily on bioactivity-guided chromatographic separation, which is both time-consuming and costly.

The Belay strategy is molecularly based on the hypothesis that phytochemicals from celery could interfere with the VKORC1 line and cause inhibition of the vitamin K cycle process. There have been reports of 3D models of human VKORC1 and enzymatic states that are functionally related to this protein. The models developed for hVKORC1 metastable states and their validation through *in silico* and in vitro screening have resulted in a conceptually plausible mechanism for enzymatic reactions based on a sequence array of hVKORC1-activated states involved in vitamin K transformation. This mechanism was found to be responsible for the transformation of vitamin K.[8]

Molecular docking and molecular dynamics techniques are widely used as virtual screening tools and bond stability analysis to predict certain ligands in stably binding to target proteins. These techniques, in turn, help lead to optimization and deployment in target identification. Moreover, computational approaches such as molecular docking simulation and molecular dynamics are adopted mainly to screen potential drugs and molecules from various databases and libraries, saving experimentation costs and time in drug discovery.[9–12]

This research aims to study the affinity, interaction pattern, and stability complex of chemical compounds in celery leaves (*Apium graveolens* L.) on the structure of the VKORC1 enzyme as a candidate lead compound anticoagulant. We began by searching the literature for plant isolates before moving on to molecular docking and molecular dynamics. Lead compound candidates were assessed through binding affinity (ΔG and Ki values), binding mode, and MMGBSA.

Materials and Methods

The hardware used was a personal computer with the following specifications: AMD® Ryzen9 3900X central processing unit (CPU), Nvidia® GTX 1080 Ti graphics processing unit (GPU), 32 GB of random-access memory (RAM), and a dual system operating Ubuntu 16.04 LTS and Windows 10 Pro-64-bit for molecular docking and MD simulations.

Preparation of ligands' three-dimensional structure and pharmacochemical properties

This study used 23 compounds isolated from celery leaves that have been reported in several publications. The 3D structure of this compound was downloaded in *.sdf format from the RCSB Protein Data Bank (PDB) website (https://pubchem.ncbi.nlm.nih.gov/). This format was next converted to *.pdb files using Discovery Studio 2016. Then, the physicochemical properties were observed using the Lipinski Rule of Five, including parameters such as log P, molecular weight, number of H bond donors, number of H bond acceptors, and molar refractivity (MR).

Preparation of the VKORC1 protein's three-dimensional structure

The 3D crystal structure of the VKORC1 protein (PDB ID 6WV3) was downloaded from the RCSB Protein Data Bank (PDB) (https://pubchem.ncbi.nlm.nih.gov/) in *.pdb. With the Discovery Studio 2016 application, the native ligand, water molecules, solvents, and other non-standard residues were taken out of this structure.

Validation of the molecular docking process

Molecular docking procedure validation was carried out by re-docking the crystal structure of the native ligand (SWF) into the clean VKORC1 protein structure using Autodock 4.2.6. Cleaned 3D structure of 6WV3 protein in *.pdb, moreover formerly prepared by adding molecules polar hydrogen and charge, then saved in the *.pdbqt file. To validate the docking procedure, we positioned the native ligand in the center of the grid box, and its location and size were adjusted accordingly. The settings method algorithm used the Lamarckian Genetic Algorithm and searched the docking conformation of the ligand with a number of GA runs of 100 ns and a maximum number of elevations (medium). The results of the docking procedure validation were observed in the RMSD.

Docking simulation with test ligands

The docking simulation of the test compounds was carried out using the validated parameters from the stages of docking procedure validation. All the test ligan *.pdb format changed into a file of the form *.pdbqt using the application AutoDock 4.2. Interpretation for native ligand and test ligand includes the bond-free energy (ΔG), inhibition constant (Ki), and the visualization of interactions with amino acid residues.

Molecular dynamics simulation

Molecular dynamics simulations were carried out using the AMBER version 18 application. Before the dynamics simulations molecule, first, prepare the test ligand file that was chosen from the best conformation (best poses). The molecular dynamics simulation stage includes several stages,[13] namely preparation of enzymes and ligands, making of topology and coordinates, minimization of complexes, heating, equilibration of complexes, production, and analysis of the results of molecular dynamics. After the preparation of the test ligand and protein files, the topological preparation of the protein and the test ligand were then combined into a single complex. The complex was then enclosed in a *grid box* and followed by the addition of water solvents and ions such as (Na^+, K^+, Ca^{2+}, Cl^-, and H^+) to reach a neutral state. This complex system was carried out three times. Step in energy minimization, including the first stage, was the minimization of water molecules by as many as 1000 steps, the second stage being the minimization of the entire ligand-enzyme system and water molecules by as many as 1000 steps, and the third covering the entire system topology.

Furthermore, heating was done in a gradient, beginning at a temperature of 0-100 K, progressing to a temperature of 100-200 K, and finally to a temperature of 200-310 K. The final stages were the production process with an interval of 100 ns after the system equilibrated this complex. The results of the molecular dynamics simulation were then analyzed using the RMSD, RSMF, MMGBSA, and decomposition.

Results and Discussion

In silico drug design methods are emerging as an important tool for designing novel proteins or drugs in the fields of biotechnology and pharmaceutical drug development. These bioinformatics methods have been of great importance in the target identification and prediction of novel drugs against various human diseases.[14] Thus, the present study attempted to evaluate the screening of phytochemicals from celery against the VKORC1 protein using molecular docking and molecular dynamics to find out the potential lead compound.

VKORC1 three-dimensional structure

Vitamin K antagonists are widely used anticoagulants that target vitamin K epoxide reductases (VKORC1), a family of integral membrane enzymes. The 3D crystal structure of the VKORC1 protein (PDB ID 6WV3) contains a 155 amino acid chain with native ligand (SWF) and OLC; besides that, it is also bound to a water molecule.[15] The homo sapiens species has the property from which this protein is derived, and the 3D structure model of this protein degenerated using the X-ray diffraction method with a resolution of 2.20 Å. Several parameters influence code selection, including method (X-ray Diffraction), organism (Homo sapiens), and resolution of <2 Å. The search results show targets with code 6WV3 that meet the requirements of the three parameters. Only clean VKORC1 protein structures were used in the docking simulation (Figure 1a).

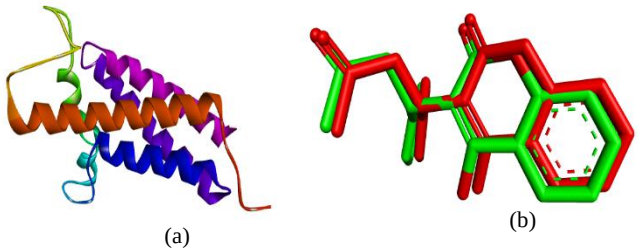

(a) (b)

Figure 1: 3D visualization of macromolecules and ligands: the VKORC1 protein's experience (a) Macromolecule VKORC1 (6WV3) and (b) Overlapping native ligand overlap crystallography X-rays with best native ligand poses (SWF).

ISSN 2616-0684 (Print)
ISSN 2616-0692 (Electronic)

Filtering the test ligands

Twenty-three compounds previously had their pharmacochemistry properties predicted using Lipinski's rules (http://www.scfbio-iitd.res.in/software/drugdesign/lipinski.jsp) to determine their ability to cross cell membranes in the body. Lipinski's rule for oral drugs states that the compound should have properties of molecular weight <500 Da, partition coefficient (Log P) <5, number of proton hydrogen bond donors <5, number of hydrogen bond proton acceptors <10, and molar refractive index between 40 and 130.

Seventeen of the twenty-three compounds demonstrated oral drug-like properties (Table 1). S18, S19, S20, S21, S22, and S23 were the compounds with negative log P values that didn't obey the Lipinski rule. Because these six compounds did not have any negative log P values, it was predicted that they would not be able to penetrate the lipid bilayer. Suppose the compound has a log P value greater than 5. In that case, it is predicted that it will interact quickly, penetrate the lipid bilayer of the cell membrane, and be widely distributed throughout the body. As a result, drug compounds will have a higher level of toxicity.

The BM value shows that the higher the hydrogen bonding capacity, the more energy was required for the absorption process to take place. Compounds S18, S20, S21, S22, and S23 have BM values greater than 500 Da and are not expected to diffuse through the cell membrane. Similarly, the number of hydrogen bond acceptors and donors for compounds S18, S19, S20, S21, S22, S23, and S10 were thought to be strongly bound or hindered in interacting with the binding site. The MR properties of compounds S21, S22, and S23 were supposed to be weakly bound or hindered in interacting with the binding site. According to Lipinski, 17 compounds will be evaluated further in molecular docking (Table 1).

Table 1: Lipinski-based physicochemical properties of the test ligands

Entry	Test Ligand	Log P	Molecular Weight (Dalton)	Number of H bond acceptors	Number of H bond donors	MR (Molar Refractivity)	ΔG (kcal/mol)	Ki (nM)
S1	6–Isopentenyloxy–isobergaptene	3.718	300	5	0	75,8089	-9.27	0.161
S2	Heratomin	3.709	270	4	0	82,3609	-9.26	0.162
S3	*Apigenins*	2.419	270	5	3	70,8138	-9,22	0.175
S4	Lanatine	3.709	270	4	0	75,8089	-9,13	0.202
S5	*Isoimperatorin*	3.709	270	4	0	75,8089	-8.94	0.282
S6	Oxypeucedanin	2.921	286	5	0	75,3299	-8.91	0.348
S7	*Kaempferol*	2.305	286	6	4	72,3856	-8.86	0.319
S8	*Luteolin*	2.125	286	6	4	72,4786	-8.81	0.351
S9	Imperatorin	3.709	270	4	0	75,8089	-8.70	0.419
S10	*Quercetin*	2.010	302	7	5	74,0504	-8.64	0.465
S11	Chrysoeriol	2.428	300	6	3	77,3658	-8.40	0.694
S12	*Ɣ-Selinene*	4.869	204	0	0	66,8129	-8.09	1.18
S13	*Δ-Selinene*	4.869	204	0	0	66,8129	-8.00	1.37
S14	*(s) rutaterin*	1.398	262	5	2	67,1935	-7.95	1.49
S15	*A-Selinene*	4.725	204	0	0	66,7429	-7.91	1.59
S16	*Apiumetin*	2.204	244	4	1	65,7097	-7.87	1.71
S17	*Osthenol*	2.833	230	3	1	65,9107	-7.78	1.97
S18 *	*luteolin 7-O-β-D-apiofuranosyl-β-D-glucopyranoside*	-2.087	580	15	9	131,1621		
S19 *	*luteolin 7-O-β-D glucopyranoside*	-0.401	448	11	7	105,2090		
S20 *	*apigenin 7-O-β-D-apiofuranosyl(1→2)-β-D-glucopyranoside*	-1.792	564	14	8	129,4973		
S21 *	*chrysoeriol 7-O-β-D-apiofuranosyl(1→2)*	-1.784	594	15	8	136,0493		

S22 *	*-β-D-glucopyranoside luteolin 7-O-[β-D-apiofuranosyl(1→2)-(6''-O-malonyl)]-β-D-glucopyranoside*	-2.061	666	18	9	147,2882
S23 *	*apigenin 7-O-[β-D-apiofuranosyl(1→2)-(6''-O-malonyl)]-β-D-glucopyranoside*	-1.767	650	17	8	145,6234

*There was no molecular docking simulation.

Validation of the molecular docking process

Docking procedure validation was carried out by re-docking native ligands to their macromolecules. The purpose of validating the docking procedure was to determine the binding site of the native ligand with the target protein so that valid parameters are obtained for docking the test compound/ ligand. The parameters of the docking procedure validation are shown by the RMSD (Root Mean Square Deviation) value ≤ 2Å, indicating that the docking method used has a small deviation and can be used for docking simulations. The docking procedure method uses the coordinates and size of the grid box of X= −10.742, Y= 27.718, and Z = 55.762 and 50×42×44, respectively. Other parameters included a grid spacing of 0.375 Å and the Lamarckian Genetic Algorithm as the algorithm method. The docking conformation search was set to run 100 times in a single belay with a medium evaluation. The best-pose of native ligand (Fig. 1b) have RMSD values, energies (ΔG), and constant inhibition (Ki) of −10.91 kcal/mol, 0.452 nM, and 0.45 Å, respectively. The RMSD value obtained indicates that the coordinates and sizes of the grid box used in the docking simulation for the test compounds were acceptable.

Ligands interaction with the structure of the VKORC1

The calculated docking score was used to analyze docking results and identify preferential binding sites. The docking simulation results were represented as bond-free energy values (ΔG), inhibition constants (Ki), and interaction patterns formed between the ligand and the target protein (Table 1 and Figure 2). Bond-free energy (ΔG) shows the ability of the ligand to interact with the binding site of the protein, where a lower value ΔG indicates stronger interaction skills. The Ki value indicates affinity between the ligand and the binding site of the protein.[16] The interaction between the ligand and the VKORC1 binding site was visualized by using a variety of different types of interactions, including hydrogen bonds, van der Waals interactions, and hydrophobic interactions such as pi-alkyl, alkyl, and pi-sigma. A significant contribution to anticoagulation activity is made by the amino acid residues asparagine 80 and tyrosine 139.[17]

The interaction between the VKORC1 structure and the native ligand (SWF) involves 19 amino acid residues in the protein's active site. These interactions formed three-bond hydrogen with amino acid residues ASN80, TYR139, and GLY60, as well as bond hydrophobicity and Van der Waals interactions (Figure 2). Molecular docking simulation results show that all ligands were able to interact with the binding site of the VKORC1 protein structure due to having ΔG value < 0. All test ligands were capable of forming bonds with the amino acid residues Tyr139 and Asn80. However, thus far, none of the test ligands with G and Ki was stronger than the native ligand.

The lower the Ki value, the stronger the bond between the test compound and the protein; thus, the test compound has a higher activity potential than the other test compounds. Ligands S1, S2, S3, S4, and S5 have an affinity (lowest G and Ki values) and will be used in the dynamics simulation molecule to observe the stability interaction with the VKORC1 enzyme structure.

Complex stability interactions VKORC1-ligands

Simulations of molecular dynamics were carried out between the structure of the VKORC1 enzyme, the native ligand, and the structures of the top-five test ligands, which are denoted by the letters S1, S2, S3, S4, and S5. The purpose of running this simulation was to collect data from the five ligands that are part of the complex that stabilizes the structure of the VKORC1 enzyme. The Amber 18 software was used to run a molecular dynamics simulation for one hundred nanoseconds while monitoring the parameters RMSD, RMSF, MMGBSA, MMPBSA, and Decomposition.

a. RMSD

The root means square deviation, also known as RMSD, is a measurement that is frequently utilized in three-dimensional molecular geometry as a ratio of conformational change of the molecule. An RMSD analysis was performed to ensure that the structural stability of the protein-ligand complex was maintained throughout the simulation and to describe how much the state of the complex ligands changed from the beginning to the end of the simulation.

The RMSD analysis performed on the native ligand reveals that throughout the entirety of the simulation, it remained relatively constant and did not exhibit any spikes at any point. In the meantime, looking at the graph, it appears that the protein is stable from the beginning of the simulation until it reaches 35 ns. At 48 ns, it began to experience a spike, and after that time, it began to gradually return to its previous level until the end of the simulation. On the test ligands, S1 and S2 show profile RMSD movement that was comparable from the beginning to the end of the simulation. This indicates that the RMSD profile tends to remain constant and does not experience a spike. In a similar vein, the protein appears to have maintained its original state throughout the entirety of the simulation.

The next ligand to be examined was ligand S3, in which the conformation of the ligand changes position after 20 ns and remains in that state until the end of the simulation, with an RMSD of approximately 1 Å. While the simulation was being run on the protein, up to 5 ns of RMSD increased to 2.5 Å at the beginning of the simulation, and the RMSD values remained constant at this value throughout the simulation, with only a small amount of change occurring in the RMSD value at the end of the simulation. In addition, the RMSD for the ligand S4 was stable from the beginning of the simulation until it spiked at 44 ns, and then it remained constant until the end of the simulation. RMSD, on the other hand, showed that the protein was unstable at ten nanoseconds, but then it became stable again up to 90 nanoseconds, and then it spiked again at the end of the simulation. In addition, the RMSD of the S5 test ligand appears to be stable and does not change significantly from the beginning to the end of the simulation. The same thing occurred with RMSD; the protein appeared stable right from the start of the simulation through its conclusion. In general, the RMSD value for all of the test ligands was less than two, and the RMSD value for proteins was less than five (Figure 3). It is possible to conclude from these two parameters, that all five test ligands, in addition to the native ligand, were capable of stabilizing the complex.

ISSN 2616-0684 (Print)
ISSN 2616-0692 (Electronic)

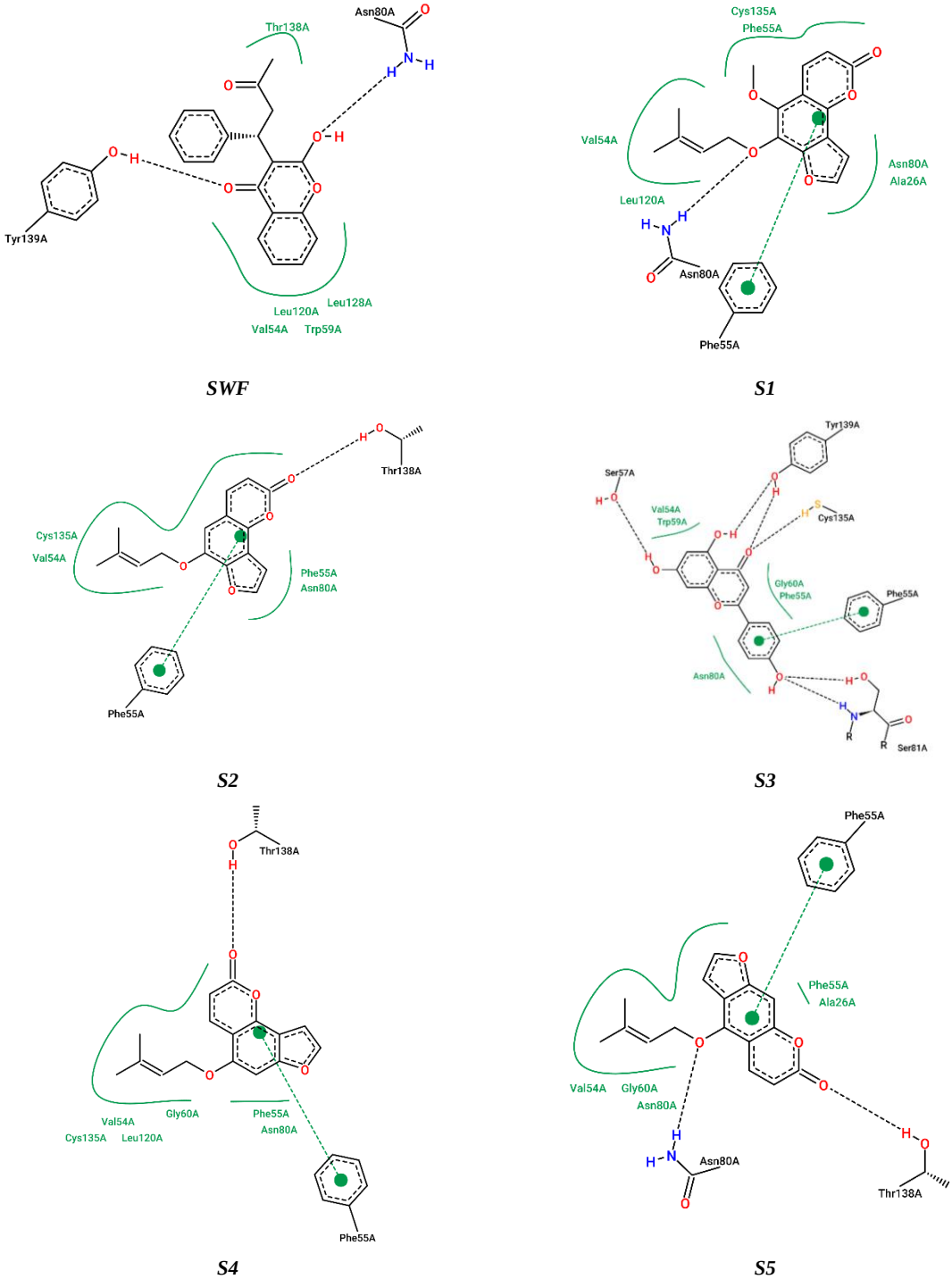

Figure 2: Typical 2D visualization of ligand interaction in the VKORC1 protein binding site.

b. RMSF

The root means square of fluctuations, or RMSF, is a measure of the deviation between a particle's position and some of its reference positions. This deviation is expressed as a square root. To determine the extent to which the fluctuations in the movement of each amino acid residue in C-alpha during the simulation were carried out, the RMSF value was calculated for each amino acid residue in C-alpha. This allows one to see how far each amino acid residue in C-alpha moved during the simulation (15).

Due to the area's high RMSF value, it can be deduced that this region contains flexible residue. Because the helical structure of a protein, of which flexible residues are a part, does not rely on hydrogen bonds to maintain its shape, the flexible residues are free to move around within the protein. The RMSF of all ligands to the Asn80 and Tyr139 amino acid residues shows RMSF values of 0.58-1.07 and 0.60-0.64 Å, respectively (Figure 4). Significant amino acid fluctuations occur at amino acid residues of 35, 47, 70, 100, and 127 with an average RMSF of 2.2; 2,2; 4; 2; and 3 Å, respectively. These fluctuations do not play an important role in the stability of the interaction, which was determined by fluctuations around Asn 80 and Tyr139 amino acid residues. It shows that move all ligands still stable in position (RMSF < 2.0Å) to important amino acid residues.

ISSN 2616-0684 (Print)
ISSN 2616-0692 (Electronic)

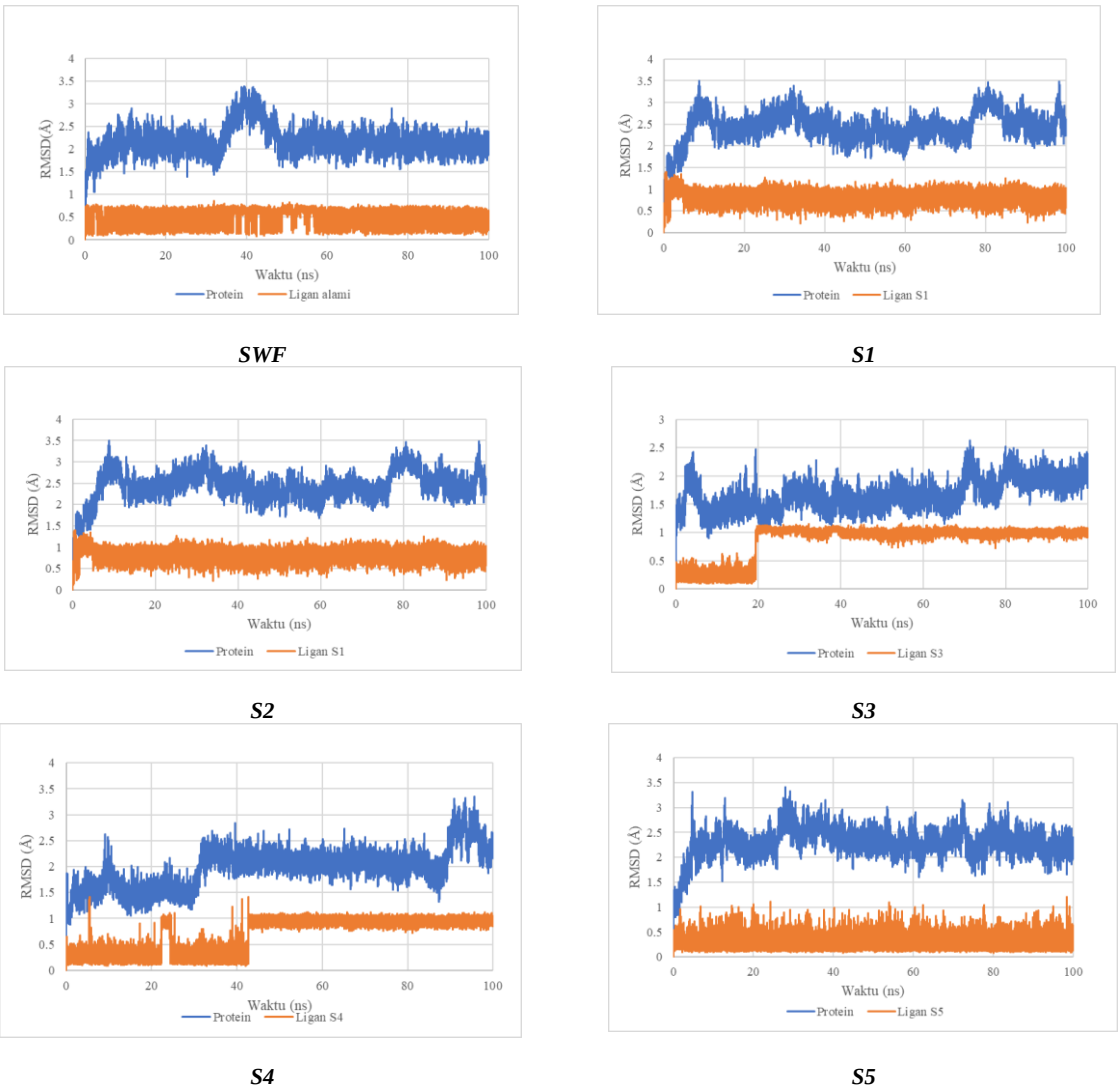

Figure 3: Variations in RMSD for both native and test ligands.

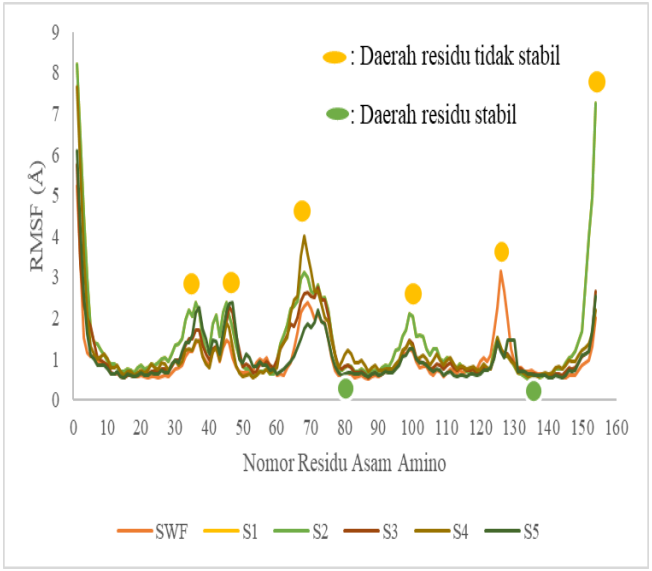

Figure 4: Fluctuations in the residue surrounding the bonding atom.

c. Quantification of hydrogen bonds

Hydrogen bonds are bonds that occur between hydrogen atoms in one molecule and one of the elements (N, O, or F) in another molecule, which is the strongest dipole-dipole force.[18] The conformational fraction of participating residues that is indicated by the presence of at least one hydrogen bond that involves a residue is referred to as the hydrogen bond occupancy.

The results of the analysis of the percentage of hydrogen bond occupancy in native ligand showed the highest occupancy value was at the amino acid Asn79 as a donor, with a value of 0.29%. The ligand S1 showed the highest occupancy on the amino acid Ala25 as a donor, with a value of 39.67%. The ligand S2 showed the highest occupancy on the Asn79 amino acid as a donor, with a value of 7.92%. The ligand S3 showed the highest occupancy on the Ser56 amino acid as an acceptor, with a value of 72.47%. The ligand S4 showed the highest occupancy on the Asn79 amino acid as a donor, with a value of 1.72%. The ligand S5 showed the highest occupancy on the Ser80 amino acid as a donor, with a value of 0.83%. A hydrogen bond was said to be strong if the occupancy value was ≥ 80%, and declared stable if the occupancy value was ≥ 50%.[19] The results of this analysis indicate the formation of stable hydrogen bonds throughout the simulation in the ligand S3 (Figure 5). This result has a correlation with the molecular docking results (Figure 2), where the value of hydrogen bonds indicating stable occupancy was found in the complex S3. This indicates that during the molecular

ISSN 2616-0684 (Print)
ISSN 2616-0692 (Electronic)

dynamics simulations, there was a large movement between the protein and the ligand.[10,20]

d. MMGBSA

MMGBSA is a popular approximation method for estimating the free energy of binding of macromolecules and ligands.[21] The MMGBSA calculation method includes components of *van der Waals* energy (E_{VDW}), electrostatic energy (E_{EL}), Electrostatic to Solvation Free Energy (E_{GB}), Non-polar to Solvation Free Energy (E_{SURF}), ΔG_{gas}, $\Delta G_{solv,}$ and total bond-free energy (ΔG_{totals}). The greater the negative value of the bond-free energy (ΔG), the greater a compound's ability to bind to the protein it is associated with.

Van der Waals energy (E_{VDW}) contributes much to making MMGBSA complex energy for all ligands. This corresponds to the van der Waals energy of native ligand (SWF) with energy as big -49.0176 kcal/mol. While the ligand S1 showed more negative energy than energy as big -44.6267 kcal/mol. Non-covalent interactions between molecules and atoms or molecules are important in defining overall binding affinities and associated conformational changes in a variety of key processes, such as protein-drug interactions and drug development, as well as charge-transfer mechanisms in optoelectronic materials.[22] Interestingly, the ligand S3 though having E_{VDW} was the most positive but had the most negative EEL with an energy of -19,859 kcal/mol. Overall, the ligand S1 has the most negative total energy with an energy of -43.7432 kcal /mol (Figure 6). So that this ligand was capable of forming a more stable complex compared to the native ligand.

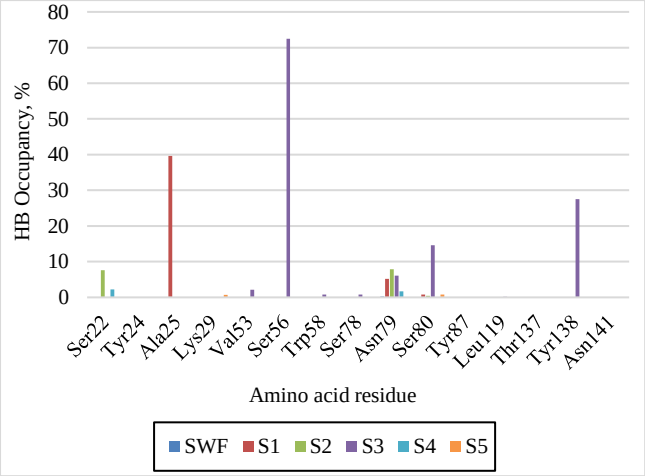

Figure 5: Analysis of the occupancy of hydrogen bonds.

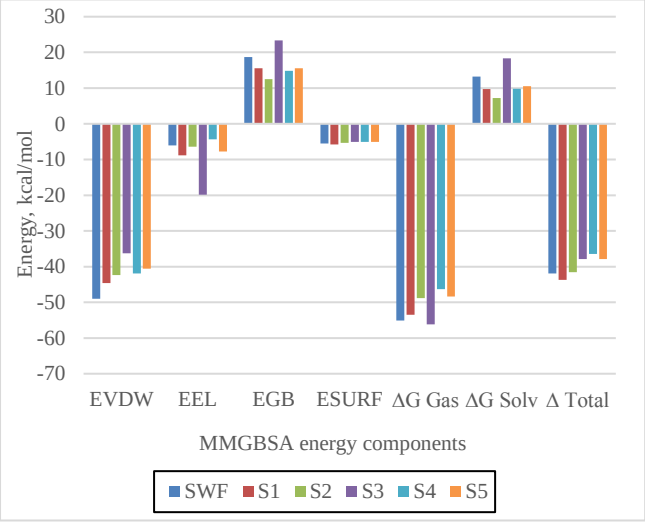

Figure 6: Displaying the component MMGBSA energy for the complexes in a plot.

e. Decomposition

The MMGBSA calculation method was utilized in the process of carrying out the decomposition analysis. Through decomposition analysis, it is possible to determine which residues help the protein bind to ligands well. Intermolecular interactions were formed between the native ligand (SWF) and the amino acids Leu21, Ser22, Ala25, Val53, Phe54, Phe62, Phe82, Phe86, Tyr87, and Leu119, Val133, Asn79, Ser80, and Tyr137. On the other hand, ligand S1 established intermolecular connections with the amino acids Ser22, Tyr24, Ala25, Val53, Phe54, Trp58, Gly59, Ser78, Asn79, Ser80, Leu119, Ile122, Leu123, Val133, Cyx134, Thr137, and Tyr138. Similarly, ligand S2 formed intermolecular interactions with the amino acids Leu119, Ile122, Leu123, Cys134, and Thr137. These amino acids included Ser22, Ala25, Val53, Phe54, Ser56, Trp58, Gly59, Phe62, Asn79, Ser80, and Leu119. The amino acids Ala25, Leu26, Lys29, Val53, Phe54, Ser56, Trp58, Gly59, Ser78, Asn79, Ser80, Leu119, Leu123, Cyx134, and Tyr138 formed intermolecular interactions with the ligand S3. The amino acids Ala25, Lys29, Val53, Phe54, Ser56, Trp58, Gly59, Asn79, Ser80, Leu119, Ile122, Leu123, and Cys134 were involved in the formation of intermolecular interactions with the ligand S4. The amino acids Ala25, Lys29, Val53, Phe54, Ser56, Trp58, Gly59, Asn79, Ser80, Leu119, Ile122, Leu123, and Cys134 formed intermolecular interactions with the ligand S5. In general, every ligand that was put to the test continued to affect the Asn80 and Tyr139 amino acid residues (Figure 7). This demonstrates that the ligand continues to form the bond corresponding to the initial position obtained from the MD simulation.

According to the findings of the molecular dynamics analysis, it demonstrated a satisfactory level of RMSD stability across all five complexes (S1, S2, S3, S4, and S5). RMSF shows that the five complexes confirmed that the amino acid residues on the active side, specifically Asn80 and Tyr139, were in a stable position with an RMSF value below 2Å. This was shown by the fact that the RMSF value was less than 2 Å. The analysis of hydrogen bonds reveals that the S3 complex was stable, with the highest occupancy percentage of 72.47% in the Ser56 amino acid residue. According to the calculations done with the MMGBSA, complex S1 was the one that possessed a favorable affinity and had a total energy component (ΔG) value of –43.7432 kcal/mol. In terms of decomposition, complexes S1, S2, and S3 were the ones that were determined to be stable. By "stable," we mean that they correlated the docked amino acid residues with the outcomes of the molecular dynamics simulations. S1 was chosen as the lead compound because it was the only one that could keep the complex stable while the molecular dynamics simulations were being run, and it also has the potential to become a candidate for the guiding compound to be used as an anticoagulant.

Conclusion

The five test ligands with ligand codes S1, S2, S3, S4, and S5 with ΔG values of –9.27, –9.26, –9.22, –9.13, and –8.94 kcal/mol, respectively, were determined to interact most effectively with the VKORC1 enzyme based on the results of a docking simulation involving 17 test compounds. The five complexes in RMSD and RMSF exhibit stable fluctuation values for a period of more than 100 ns, which was consistent with the theory of molecular dynamics. The ligand S1 (6-isopentenyloxy-isobergapten) exhibited the most negative MMGBSA value (ΔG) of –43.7432 kcal/mol. Therefore, 6-isopentenyloxy-isobergapten has the potential to be a candidate for a lead compound.

Conflict of Interest

The authors declare no conflict of interest.

Authors' Declaration

The authors hereby declare that the work presented in this article is original and that any liability for claims relating to the content of this article will be borne by them.

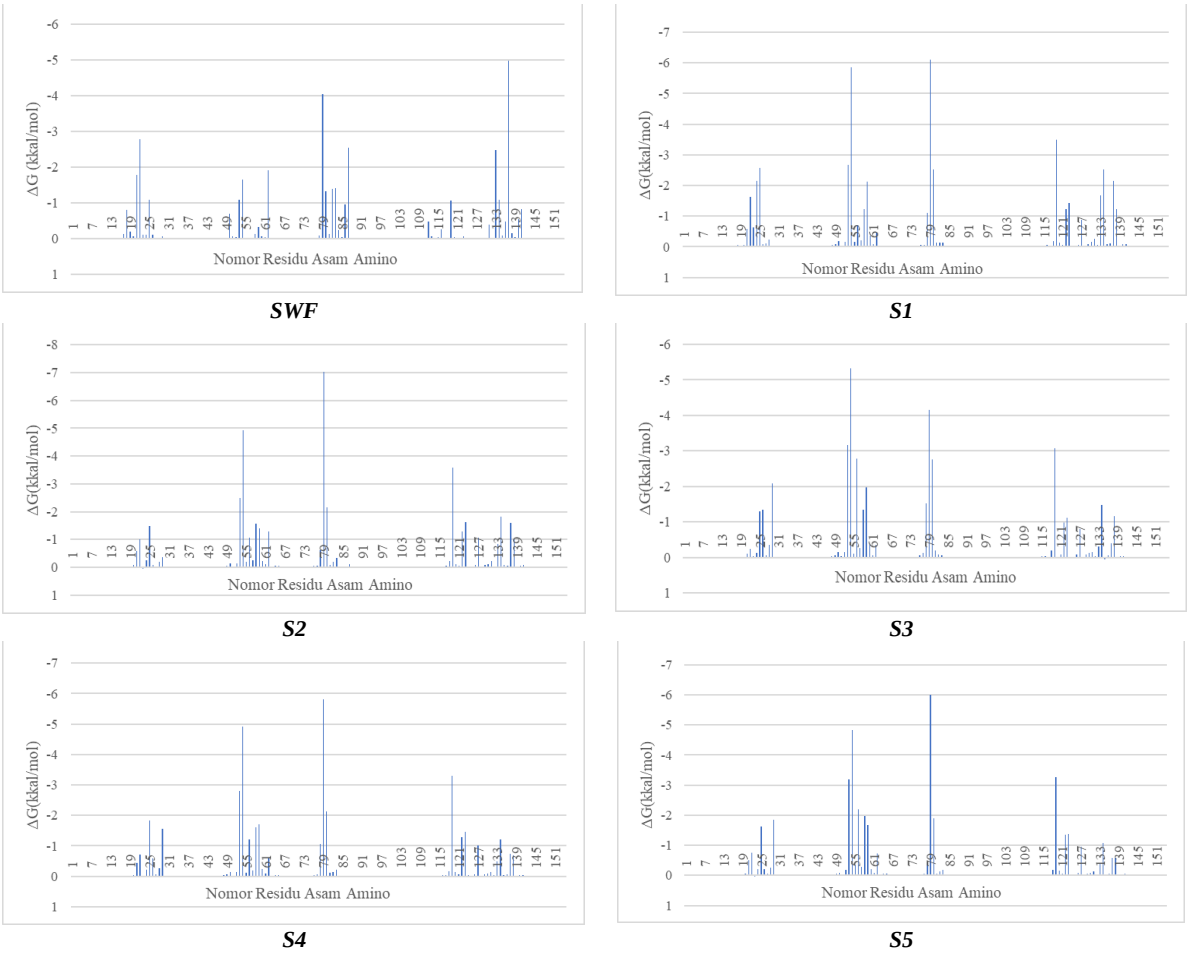

Figure 7: Presenting the decomposition of the complexes in the form of a plot.

References

1. Saner FH, Kirchner C. Monitoring and Treatment of Coagulation Disorders in End-Stage Liver Disease. Visc Med. 2016;32(4):241-248. doi:10.1159/000446304
2. Laslett LJ, Alagona P, Clark BA, Drozda JP, Saldivar F, Wilson SR, Poe C, Hart M. The worldwide environment of cardiovascular disease: Prevalence, diagnosis, therapy, and policy issues: A report from the american college of cardiology. J Am Coll Cardiol. 2012;60(25 SUPPL.). doi:10.1016/J.JACC.2012.11.002
3. Gbyli R, Mercaldi A, Sundaram H, Amoako KA. Achieving Totally Local Anticoagulation on Blood Contacting Devices. Adv Mater Interfaces. 2018;5(4):1700954. doi:10.1002/ADMI.201700954
4. Johnson JA, Gong L, Whirl-Carrillo M, Gage BF, Scott SA, Stein CM, Anderson JL, Kimmel SE, Lee MTM,Pirmohamed M, Wadelius M, Klein TE, Altman RB. Clinical pharmacogenetics implementation consortium guidelines for CYP2C9 and VKORC1 genotypes and warfarin dosing. Clin Pharmacol Ther. 2011;90(4):625-629. doi:10.1038/clpt.2011.185
5. Sikka P, Bindra VK. Newer antithrombotic drugs. Indian J Crit Care Med. 2010;14(4):188-195. doi:10.4103/0972-5229.76083
6. Guven H, Arici A, Simsek O. Flavonoids in our foods: a short review. J Basic Clin Heal Sci. 2019;3(2):96-106.
7. Rumpho ME, Edwards GE, Loescher WH. A Pathway for Photosynthetic Carbon Flow to Mannitol in Celery Leaves. *Plant Physiol*. 1983;73(4):869-873. doi:10.1104/PP.73.4.869
8. Chatron N, Chalmond B, Trouvé A, Benoit E, Caruel H, Lattard V, Tchertanov L. Identification of the functional states of human Vitamin K epoxide reductase from molecular dynamics simulations. RSC Adv. 2017;7(82):52071-52090. doi:10.1039/C7RA07463H
9. Nursamsiar, Nur S, Febrina E, Asnawi A, Syafiie S. Synthesis and Inhibitory Activity of Curculigoside A Derivatives as Potential Anti-Diabetic Agents with β-Cell Apoptosis. J Mol Struct. 2022;1265. doi:10.1016/J.MOLSTRUC.2022.133292
10. Asnawi A, Aman LO, Nursamsiar, Febrina E. Molecular Docking and Molecular Dynamic Studies: Screening Phytochemicals of Acalypha Indica Against Braf Kinase Receptors For Potential Use In Melanocytic Tumours. Rasayan J Chem. 2022;15(2):1352-1361. doi:10.31788/RJC.2022.1526769
11. Febrina E, Asnawi A, Abdulah R, Lestari K, Supratman U. Identification of Flavonoids From Acalypha Indica L. (Euphorbiaceae) as Caspase-3 Activators Using Molecular Docking and Molecular Dynamics. Int J Appl Pharm. 2022;14(Special issue 5):162-166. doi:10.22159/IJAP.2022.V14S5.34
12. Ischak NI, Ode LA, Hasan H, Kilo A La, Asnawi A. In silico screening of Andrographis paniculata secondary metabolites as anti-diabetes mellitus through PDE9 inhibition. Res Pharm Sci. 2023;18(1):100. doi:10.4103/1735-5362.363619
13. Febrina E, Alamhari RK, Asnawi A, Abdulah R, Lestari K, Levita J, Supratman U. Molecular Docking and Molecular Dynamics Studies of Acalypha Indica L. Phytochemical Constituents with Caspase-3. Int J Appl Pharm. 2021;13(Special Issue 4):210-215. doi:10.22159/IJAP.2021.V13S4.43861
14. Ritchie TJ, McLay IM. Should medicinal chemists do molecular modelling? Drug Discov Today. 2012;17(11-12):534-537. doi:10.1016/J.DRUDIS.2012.01.005
15. Liu S, Li S, Shen G, Sukumar N, Krezel AM, Li W. Structural basis of antagonizing the vitamin K catalytic cycle for anticoagulation. Science *(80-)*. 2021;371(6524). doi:10.1126/SCIENCE.ABC5667
16. Nursamsiar, Asnawi A, Kartasasmita RE, Ibrahim S, Tjahjono DH. Synthesis, biological evaluation, and docking analysis of methyl hydroquinone and bromo methyl hydroquinone as potent cyclooxygenase (COX-1 and COX-2) inhibitors. J Appl Pharm Sci. 2018;8(7):16-20. doi:10.7324/JAPS.2018.8703

17. Wu S, Chen X, Jin DY, Stafford DW, Pedersen LG, Tie JK. Warfarin and vitamin K epoxide reductase: a molecular accounting for observed inhibition. Blood. 2018;132(6):647. doi:10.1182/BLOOD-2018-01-830901
18. Weinhold F, Klein RA. What is a hydrogen bond? Resonance covalency in the supramolecular domain. Chem Educ Res Pract. 2014;15(3):276-285. doi:10.1039/C4RP00030G
19. Cetin E, Atilgan AR, Atilgan C. DHFR Mutants Modulate Their Synchronized Dynamics with the Substrate by Shifting Hydrogen Bond Occupancies. J Chem Inf Model. Published online December 26, 2022. doi:10.1021/acs.jcim.2c00507
20. Xie H, Li Y, Yu F, Xie X, Qiu K, Fu J. An investigation of molecular docking and molecular dynamic simulation on imidazopyridines as B-raf kinase inhibitors. Int J Mol Sci. 2015;16(11):27350-27361. doi:10.3390/ijms161126026
21. Genheden S, Ryde U. The MM/PBSA and MM/GBSA methods to estimate ligand-binding affinities. Expert Opin Drug Discov. 2015;10(5):449-461. doi:10.1517/17460441.2015.1032936
22. Mahmudov KT, Kopylovich MN, Guedes da Silva MFC, Pombeiro AJL. Non-covalent interactions in the synthesis of coordination compounds: Recent advances. Coord Chem Rev. 2017;345:54-72. doi:10.1016/J.CCR.2016.09.002

.